Journal of Integrative Agriculture 2026, 25(2): 709–720

Available online at ScienceDirect

Journal of Integrative Agriculture



RESEARCH ARTICLE

Candidate gene analysis of cabbage head-splitting resistance based on QTL mapping and omics profiling

Xiaowei Zhu[1*], Min Wang[1*], Xiang Tai[1], Panling Lu[1], Hang Gui[2], Jinxiu Chen[1#], Tianyue Bo[1#]

[1] *Shanghai Key Laboratory of Protected Horticultural Technology, Protected Horticultural Research Institute, Shanghai Academy of Agricultural Sciences, Shanghai 201403, China*

[2] *Shanghai Shengeng Agricultural Development Co., Ltd., Shanghai 201824, China*

Highlights

- Head-splitting resistance QTL(s) in cabbage were investigated using an F_2 population derived from a cross between ZF and '103'.
- One head-splitting resistance QTL, *qNLQ3.1*, was identified through multiple approaches including QTL-seq, Graded Pool-seq (GPS), and traditional genetic linkage analysis.
- Integration of transcriptomic and metabolic profiling enabled the identification of *Bol028000* as a plausible candidate gene within *qNLQ3.1*.

Abstract

Head-splitting is a prevalent physiological disorder in cabbage that causes substantial economic losses. However, the genetic factors and molecular mechanisms underlying head-splitting resistance remain largely unexplored. This study identified a genomic region (*qNLQ3.1*) for head-splitting resistance on chromosome C03 through the combination of QTL-seq and GPS analysis in an F_2 population derived from hybridizing two cabbage inbred lines, 'Dazhengfu' (ZF, susceptible) and '103' (resistant). Traditional genetic linkage analysis narrowed *qNLQ3.1* to a 74.6 kb region. Furthermore, comparative analysis of the two parental lines using transcriptomic and metabolic profiling demonstrated the crucial role of hormones in regulating head-splitting resistance. *Bol028000*, encoding a homologue of Arabidopsis Cytokinin Response Factor 3 (CRF3), emerged as a promising candidate for head-splitting resistance and was subsequently validated through Sanger sequencing and quantitative RT-PCR (qRT-PCR). Subcellular localisation analysis revealed that *Bol028000* was mainly expressed in the nucleus. Additionally, one kompetitive allele-specific PCR (KASP) marker from *Bol028000* was developed and utilized to screen 42 inbred lines. These findings enhance the theoretical understanding of head-splitting resistance and provide valuable insights for the molecular breeding of head-splitting resistant cabbages.

Keywords: cabbage, head-splitting resistance, QTL, transcriptomic and metabolic profiling

1. Introduction

Cabbage (*Brassica oleracea* L. var. *capitata*) is a globally cultivated *Brassica* vegetable of significant importance. The leafy head, which serves as the storage organ of cabbage, is harvested for consumption. The appearance and quality of cabbage heads are frequently hampered by splitting, which occurs predominantly in the late heading stage and results in considerable economic losses. In most production regions, head-splitting is typically mitigated through optimization of agronomic practices, including modification of planting and harvesting schedules and reduction of irrigation and fertilization during late-stage cultivation. As these measures cannot completely prevent head-splitting, the development of resistant cultivars remains the most effective management strategy.

Cabbage resistance to head-splitting is a complex genetic trait controlled by multiple loci and is easily influenced by environmental factors (Chiang 1972; Zeng *et al.* 2011; Su

Received 28 October 2024; Received in revised form 14 March 2025; Accepted 14 May 2025; Available online 14 November 2025
[#]Correspondence Jinxiu Chen, E-mail: cabbagecjx@126.com; Tianyue Bo, E-mail: tybo@saas.sh.cn
[*]These authors contributed equally to this study.

© 2026 CAAS. Publishing services by Elsevier B.V. on behalf of KeAi Communications Co. Ltd. This is an open access article under the CC BY-NC-ND license (http://creativecommons.org/licenses/by-nc-nd/4.0/). Peer review under responsibility of Editorial Board of *Journal of Integrative Agriculture*.
doi: 10.1016/j.jia.2025.11.020

et al. 2012, 2019). Several studies have analyzed the bi-parental QTL of head-splitting resistance in cabbage. Six QTLs for head-splitting resistance were identified and mapped on chromosomes 2, 4, and 6 using an F_2 population derived from '748' (head-splitting resistant inbred line) and '747' (head-splitting susceptible inbred line) (Pang *et al.* 2015). Among these QTLs, two markers (BRMS137 and BRPGM0676) tightly linked to head-splitting resistance were mapped to the *SPL-2-1* QTL region (Pang *et al.* 2015). Su *et al.* (2015) identified nine QTLs for head-splitting resistance, which were distributed on chromosomes C3, C4, C7, and C9, through field evaluation of head-splitting resistance of the double haploid (DH) population derived from the cross between '79–156' (head-splitting susceptible inbred line) and '96–100' (head-splitting resistant inbred line). Using the whole-genome resequencing-based approach (QTL-seq) in an F_2 segregation population (G274×G279), we recently delimited a candidate genomic region associated with head-splitting resistance at the 45.8–51.4 Mb (5.6 Mb) region on chromosome 3 and identified a proline rich protein 4 gene (*Bol016058*) as the candidate gene from the head-splitting resistant line G279 (Zhu *et al.* 2022). We further developed a diagnostic insertion-deletion (InDel) marker based on the 45-bp insertion of *Bol016058* in G279 (Zhu *et al.* 2022). However, only seven head-splitting resistant inbred lines have been identified using the *Bol016058*-based InDel marker (Zhu *et al.* 2022). Due to the limited effects of individual loci on head-splitting resistance, identifying additional resistance genes for advanced precision breeding, such as gene editing and marker-assisted selection (MAS), is essential.

Transcriptome dynamics reveal transcriptional networks and candidate genes associated with *Brassica* traits. Sun *et al.* (2019) compared the transcriptomes of leaves from two different Chinese cabbage varieties with those of pak choi during plant development and revealed the molecular pathways involved in leafy head formation in Chinese cabbage. Additionally, Zhang K *et al.* (2022) identified a regulatory stage that initiates the heading process by fuelling transcriptional reprogramming in two *Brassica* heading crops, Chinese cabbage and cabbage, using large-scale time-series transcriptome assays. Liu X *et al.* (2020) elucidated a molecular regulatory network for cabbage resistance to *Fusarium oxysporum* f. sp. *conglutinans* (*Foc*) based on a time-resolved dual transcriptomic landscape. These findings suggest an approach to enhance understanding of head-splitting resistance in cabbage plants.

Plant hormones influence various stages of leaf development (Li *et al.* 2007; Bar and Ori 2014; Shwartz *et al.* 2016; Du *et al.* 2018; Zhao *et al.* 2021; Tabusam *et al.* 2023). A relatively high content and uneven distribution of endogenous auxin concentration improve the characteristics of leafy head formation in Chinese cabbage (He *et al.* 2000). Furthermore, genomic evidence indicates that four gene ontology categories associated with phytohormones (cytokinin (CK), auxin, gibberellin (GA), and jasmonic acid (JA)) are potential candidates for the development of *Brassica rapa* and *Brassica oleracea* leaf-heading morphotypes (Cheng *et al.* 2016). Gene transcript analysis has demonstrated that auxin transport genes *BrLAX*, *BrPIN*, and *BrPGP* likely participate in leafy head formation in Chinese cabbage (Gao *et al.* 2017). Recent forward genetic studies have identified several genes involved in leafy head development in *Brassica* species (Gao *et al.* 2020; Alemán-Báez *et al.* 2022; Huang *et al.* 2022; Zhang X *et al.* 2022). For instance, Zhang X *et al.* (2022) identified a *BrOPS* gene that regulates leaf curvature in Chinese cabbage through a brassinosteroid-dependent mechanism. However, the specific roles of plant hormones in cabbage leafy head development and their regulation of head-splitting remain to be elucidated.

In this study, we integrated QTL-seq, Graded Pool-seq (GPS), and traditional genetic linkage mapping to analyze the QTL associated with head-splitting resistance in cabbage. We conducted candidate gene analysis in the major QTL by combining single nucleotide polymorphism (SNP)/InDel annotations with transcriptomic and metabolic profiling. This analysis led to the identification of *Bol028000*, which encodes a homologue of Arabidopsis Cytokinin Response Factor 3 (CRF3), as a plausible candidate gene for head-splitting resistance. Additionally, we examined the natural occurrence of the *Bol028000* allele and explored its potential application in MAS for cabbage molecular breeding programs.

2. Materials and methods

2.1. Plant materials and phenotyping

Two cabbage inbred lines, 'Dazhengfu' (ZF) and '103', were used as parental lines in this study. ZF, a pointed head type collected from England, exhibits susceptibility to splitting after maturity, while '103', developed through system selection from the Shanghai landrace 'Heiyexiaopingtou', features a flat head and shows high resistance to splitting. Female ZF plants were crossed with male '103' plants, and the F_1 hybrids were self-pollinated to generate the F_2 segregating population. For head-splitting phenotypic data collection, the parents and F_2 were cultivated in experimental fields at the Shanghai Academy of Agricultural Sciences (Shanghai, China) during two consecutive years (Spring 2020 and 2021). A collection of 42 inbred cabbage lines, previously evaluated for head-splitting resistance in Shanghai (Zhu *et al.* 2022), was utilized to determine the polymorphism of *Bol028000*-derived Kompetitive Allele-Specific PCR (KASP) marker.

Under greenhouse conditions, natural splitting initiated approximately 71 days after planting (DAP) and continued for seven weeks until most F_2 individuals exhibited head-splitting. Head-splitting resistance was categorized based on head-splitting time using a scale of 1 to 7: 1, 0 d<head-splitting time≤7 d; 2, 7 d<head-splitting time≤14 d; 3, 14 d<head-splitting time≤21 d; 4, 21 d<head-splitting time≤28 d; 5, 28 d <head-splitting time≤35 d; 6, 35 d<head-splitting time≤42 d; 7, 42 d<head-splitting time≤49 d. Head-splitting time was defined according to Zhu *et al.* (2022).

2.2. Construction of extreme bulks and whole-genome resequencing

Genomic DNA was extracted using the CTAB method from both parents and F_2 plants from the 2020 Spring experiment for whole-genome resequencing and conventional QTL analysis. The susceptible (S-bulk) and resistant (R-bulk) bulks for head-splitting were prepared by combining equal

quantities of DNA from 20 head-splitting susceptible and 22 head-splitting resistant F_2 individuals from the 2020 Spring experiment. Illumina libraries (~350 bp) were constructed from four samples comprising the two parents, S-bulk, and R-bulk at Beijing Biomarker Technologies Co., Ltd. (Beijing, China) and sequenced using paired-end reads (150 bp×2) on an Illumina NovaSeq 6000 platform. The raw whole-genome resequencing data has been deposited in the National Center for Biotechnology Information (NCBI) Sequence Read Archive under PRJNA1222095.

2.3. QTL-seq analysis

High-quality clean reads were generated by eliminating adaptor reads, unknown sequences 'N' (reads containing unknown nucleotides>10%), and low-quality reads (reads containing>50% bases with *Q*-value≤10) from the raw sequencing data. The clean reads were aligned and mapped to the reference genome of cabbage '02-12' (*B. oleracea* var. *capitata*) in the BRAD database using BWA software (Li and Durbin 2009). SNP calling was performed using Genome Analysis Toolkit (GATK) software (McKenna *et al.* 2010). For each high-quality SNP, SNP-index and Δ(SNP-index) were calculated to identify candidate regions for head-splitting resistance (Takagi *et al.* 2013). The SNP-index, representing the proportion of reads containing SNPs different from the reference sequence, was calculated for both S-bulk and R-bulk. Δ(SNP-index) was calculated by subtracting the S-bulk SNP-index from the R-bulk SNP-index. The average SNP-index within a given genomic interval was determined using sliding window analysis with 2 Mb window size and 10 kb increment. QTL loci associated with head-splitting resistance were identified using 99% confidence intervals as the threshold.

2.4. GPS analysis

The GPS method, as described by Wang *et al.* (2019), enables rapid fine-mapping of genes through whole-genome sequencing of graded-pool samples from F_2 progeny. Clean reads from the whole-genome resequencing data of S-bulk and R-bulk were aligned against the parental ZF (head-splitting susceptible) genome sequence, followed by SNP calling. After filtering, *P*-values for each SNP were calculated using Ridit analysis with allelic frequencies from the two bulk samples. The *P*-value plot was generated using –ln(*P*-value) and chromosomal position as the *y*- and *x*-values, respectively. Background noise reduction was implemented using a non-overlapping sliding window approach, calculating the ratio of statistically significant variants (–ln(*P*-value)>10) to total variants in a ~400-kb interval. Candidate genetic intervals for head-splitting resistance were identified using a ratio plot, with peak locations representing clusters of highly linked variants of head-splitting resistance in the ~400-kb region.

2.5. QTL analysis with InDel and KASP markers in *qNLQ3.1*

The head-splitting resistance QTL identified through QTL-seq and GPS methods was validated and narrowed using novel InDel and KASP markers through traditional QTL analysis. InDel and fluorescence-based KASP markers were developed based on the variation data from QTL-seq. Primers for these markers were designed and validated in both parents. Polymorphic markers (Appendix A) were then applied to the F_2 population. Linkage analysis was performed using JoinMap 4.0 software (Van Ooijen *et al.* 2006). QTL analysis was conducted using MapQTL6.0 with the multiple QTL model (MQM mapping) procedure (Van Ooijen *et al.* 2009).

2.6. RNA-seq and quantitative RT-PCR (qRT-PCR)

Samples for RNA isolation were collected from the heading leaves of the two parents at 78 and 113 DAP during Spring 2021. At 78 DAP, most ZF individuals exhibited head-splitting, while all '103' individuals showed no splitting. The heading leaves from ZF and '103' individuals without head-splitting at 78 DAP were sampled to represent the physiological stage before head-splitting occurred. At 113 DAP, all ZF and '103' individuals exhibited head-splitting, and the heading leaves sampled at this time represented the physiological stage when head-splitting occurred. The harvested samples were immediately frozen in liquid nitrogen and stored at –80°C before RNA extraction. Three biological replicates were sampled at each time point, yielding 12 samples total (Appendix B). RNA-seq analysis, including RNA isolation, detection, cDNA library construction, and paired-end sequencing, was performed by Biomarker Technologies Co., Ltd. (Beijing, China). The raw RNA-seq data has been deposited in the National Center for Biotechnology Information (NCBI) Sequence Read Archive under PRJNA1222095.

The raw data underwent quality control processing to obtain clean data using in-house Perl scripts. For transcriptional profile analysis, clean reads were aligned to the reference genome of cabbage '02-12' using HISAT2 software (Kim *et al.* 2015). Gene expression levels were estimated by calculating fragments per kilobase of transcript per million fragments mapped (FPKM) using String Tie (v2.0.0) (Pertea *et al.* 2015). Pairwise differential expression gene (DEG) analyses were conducted using the DESeq2 package. DEGs were defined using a false discovery rate (FDR) with corrected *P*-value<0.01 and fold change (FC)≥2. Gene Ontology (GO) analysis of all DEGs was performed using ClusterProfiler (Yu *et al.* 2012). For qRT-PCR, total RNA was extracted from the same samples as RNA-seq following the MiniBEST Plant RNA Extraction Kit protocol (TaKaRa, Beijing, China). cDNA synthesis and PCR amplification were performed according to a previous study (Zhu *et al.* 2023) using gene-specific primer pairs (Appendix A). The cabbage *Actin* gene served as the internal control, with results calculated using the $2^{-\Delta\Delta Ct}$ method.

2.7. Detection of endogenous hormones

Heading leaves collected from ZF and '103' at identical time points as those for transcriptome profiling were delivered to Wuhan MetWare Biotechnology Co., Ltd. (Wuhan, China) for endogenous hormone detection (three biological replicates). Frozen heading leaves (approximately 50 mg fresh weight

per sample) were ground into powder and extracted with methanol:water:formic acid (15:4:1, v/v/v). The sample extracts were dried by evaporation under a stream of nitrogen gas, dissolved in 80% (v/v) methanol, and filtered (0.22 μm pore size) for LC-MS analysis. Hormone content determination was performed by MetWare using an AB Sciex QTRAP 6500 LC-MS/MS platform.

2.8. Phylogenetic analysis

The protein sequences homologous to Bol028000 were downloaded from the Phytozome v13 database. Multiple sequence alignments were performed using Muscle, and a phylogenetic tree was constructed using MEGA 11 software with the neighbour-joining tree method and 1,000 bootstrap replicates.

2.9. Genomic sequence comparison of *Bol028000* between ZF and '103'

The genomic sequences of *Bol028000* from ZF and '103' were amplified using gene-specific primers (Appendix A) with KOD FX Neo High-Fidelity DNA polymerase (Toyobo, Osaka, Japan), following the manufacturer's instructions. PCR fragments were submitted to Tsingke Biotechnology Co., Ltd. (Shanghai, China) for Sanger sequencing. Multiple sequence alignments were performed using DNAMAN software (Lynnon, Quebec, Canada).

2.10. Subcellular localization

To determine the subcellular localization of the Bol028000 protein, the coding sequence of *Bol028000* was amplified by PCR (for primers see Appendix A) from '103' and cloned into the pCAMBIA1300-green fluorescent protein (GFP) vector. The binary construct, in which the *Bol028000-GFP* fusion gene was controlled by the CaMV35S promoter, was introduced into *Agrobacterium tumefaciens* strain GV3101 and subsequently infiltrated into the leaves of *Nicotiana benthamiana* plants. GFP and 4′,6-diamidino-2-phenylindole (DAPI) excitation were detected using confocal microscopy (Zeiss LSM 700, Japan).

3. Results

3.1. Genetic inheritance of head-splitting resistance in '103' cabbage

The head-splitting resistant parental line '103' exhibited significantly delayed splitting compared to the susceptible line ZF (Fig. 1). Based on phenotyping data collected in Shanghai over two consecutive years, the head-splitting resistance of '103' was rated as 5 (28 d<head-splitting time≤35 d), while ZF was rated as 1 (0 d<head-splitting time≤7 d) (Fig. 1-C and D). The frequency distribution of head-splitting resistance in the two segregating populations (F_2-2020 Spring (*n*=310) and F_2-2021 Spring (*n*=698)) demonstrated continuous variation and were close to a normal distribution curve, indicating that the head-splitting resistance of '103' was quantitatively inherited (Fig. 1-C and D).

3.2. Whole-genome resequencing of cabbage

From the 310 F_2 plants (Spring 2020), 20 head-splitting susceptible and 22 head-splitting resistant plants were selected to create two extreme DNA bulks (S-bulk and R-bulk) (Fig. 1-C). Whole-genome resequencing of genomic DNA samples yielded 69.35 Gb of clean base from the four libraries (ZF, '103', S-bulk, and R-bulk). After aligning the reads to the reference genome of cabbage '02-12', ZF produced 72 million paired-end 150-bp clean reads, achieving an average depth of 16× and 89.73% 5× genome coverage, while '103' generated 70 million clean reads, resulting in an average depth of 13× and 87.84% 5× genome coverage. For S-bulk and R-bulk, 180 million and 142 million 150-bp clean reads were generated, achieving 37× and 30× sequencing depths with 95.32 and 94.95% genome coverage, respectively (Table 1). Additionally, 418,473 genome-wide SNPs were identified between S-bulk and R-bulk.

3.3. Candidate QTL for head-splitting resistance through QTL-seq

To identify QTL(s) conferring head-splitting resistance, the SNP-index of genome-wide SNPs was calculated for each bulk (Fig. 2-A and B). The Δ(SNP-index) was determined by subtracting the SNP-index of the S-bulk from that of the R-bulk and plotted against the *B. oleracea* L. var. *capitata* reference genome (http://brassicadb.cn) (Fig. 2-C). Two regions exhibiting significantly unequal contributions between the S-bulk and R-bulk were identified at 99% confidence intervals (Fig. 2-C). These regions represented candidate QTLs associated with head-splitting resistance, designated *qNLQ3.1* and *qNLQ3.2*, respectively (Fig. 2-C). *qNLQ3.1* was located on chromosome C03 from 6.38 to 9.33 Mb (2.95 Mb) (Fig. 2-C). *qNLQ3.2* was located on chromosome C03 from 13.46 to 14.34 Mb (0.88 Mb) (Fig. 2-C).

3.4. QTL validation and refinement by GPS-method

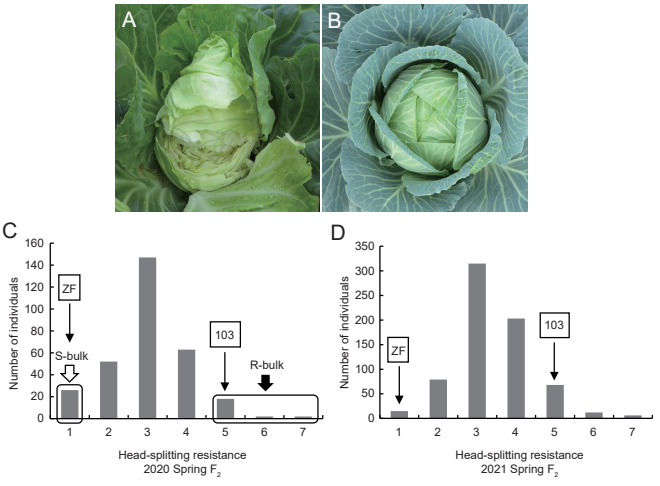


Fig. 1 Phenotypes of 'Dazhengfu' (ZF) (A) and '103' (B) and frequency distribution of head-splitting resistance grades in ZF, '103' and F_2 populations in Spring 2020 (C) and 2021 (D). ZF, head-splitting susceptible parent; '103', head-splitting resistant parent. Twenty F_2 plants with head-splitting susceptibility and 22 F_2 plants with head-splitting resistance were selected to construct susceptible and resistant bulks.

To validate the QTLs identified by QTL-seq, GPS analysis was performed on the same whole-genome resequencing data of S-bulk and R-bulk, with short reads from both bulks aligned to the ZF reference sequence. The analysis identified 4,015,558 SNPs in S-bulk and 4,072,779 SNPs in R-bulk. Ridit analysis was conducted to calculate *P*-values for each SNP (Fig. 3-A). After background noise reduction, the strongest peak was identified on chromosome C03 (Fig. 3-B). The highest ratio was observed in the physical region from 6.8 to 7.19 Mb on chromosome C03, which corresponded precisely to the candidate region of *qNLQ3.1* (Fig. 3-B). Based on the results from both methods, subsequent analysis focused on *qNLQ3.1*.

3.5. Genetic linkage analysis to validate and narrow the location of *qNLQ3.1*

To narrow down the 2.95 Mb candidate genomic region containing *qNLQ3.1*, traditional QTL mapping was performed using 300 F_2 plants grown in Spring 2020. Within the candidate interval, 51 InDel markers and 5 KASP markers were designed and screened against the parents. Eleven consistently polymorphic markers were selected for genotyping the segregating populations for QTL analysis. MQM analyses identified a major QTL for head-splitting resistance delimited by markers N2-80 and KASP4, physically located in the 7.07–7.14 Mb region on chromosome C03 (Fig. 4). The LOD values in this region ranged from 8.23 to 9.55, explaining a maximum phenotypic variation of 14.0% (Fig. 4-A). Finally, the *qNLQ3.1* locus was narrowed to a 74.6 kb physical interval on chromosome C03 (Fig. 4-C).

3.6. Comparative transcriptome analysis

To examine transcriptional regulation associated with head-splitting resistance and facilitate candidate gene identification, heading leaves were collected from both parents, ZF and '103', at 78 and 113 DAP for RNA-seq analysis. Three independent biological replicates were conducted for each heading leaf development time point, with 12 samples

Table 1 Summary of whole-genome resequencing of parents and bulks for head-splitting resistance

Sample	Clean bases	Total reads	Mapping rate (%)	5× genome coverage rate (%)	Average depth (×)
Dazhengfu (ZF)	10,792,850,182	72,111,660	90.00	89.73	16
103	10,502,869,438	70,196,400	85.60	87.84	13
S-bulk	26,880,073,208	179,595,080	82.34	95.32	37
R-bulk	21,176,205,190	141,537,678	82.90	94.95	30

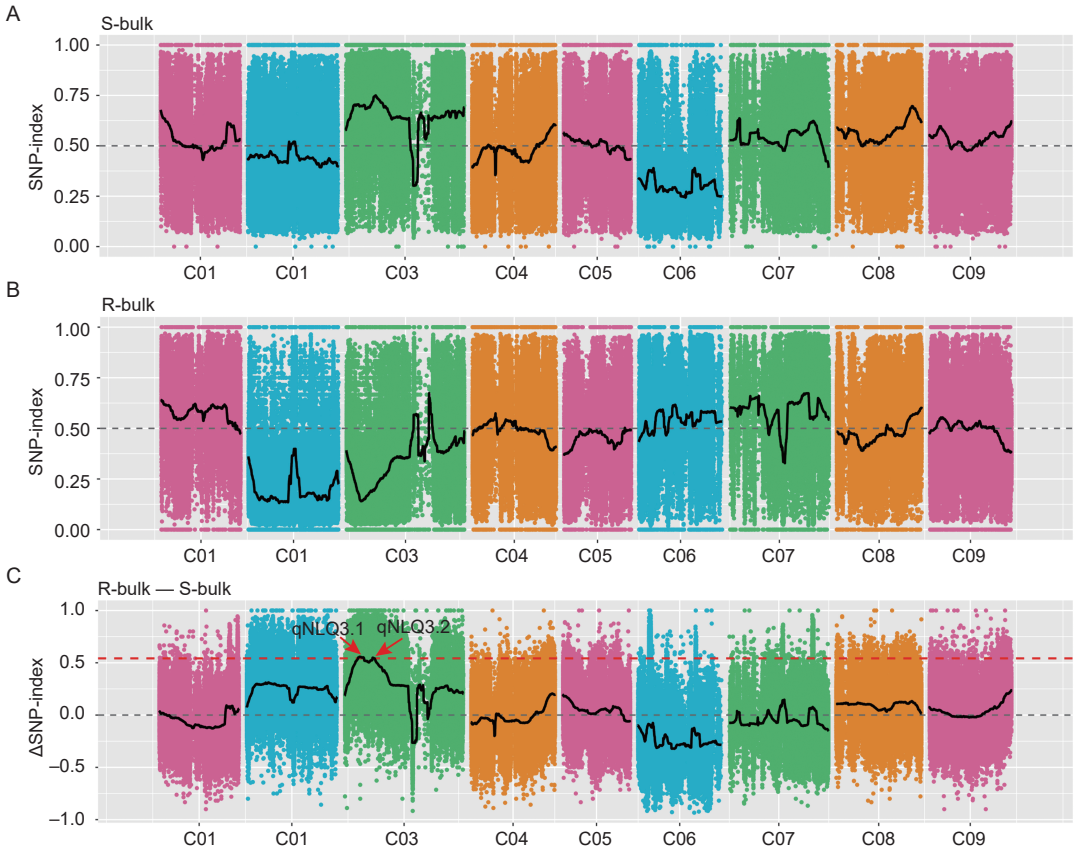


Fig. 2 SNP-index plots of the susceptible bulk (S-bulk, A) and resistant bulk (R-bulk, B), and Δ(SNP-index) (C) from QTL-seq analysis. SNP-index was calculated based on a 2-Mb interval with a 10-kb sliding window. The red dotted line is the screening threshold at a 99% confidence level. Red arrows indicate the approximate position of two candidate QTLs, *qNLQ3.1* and *qNLQ3.2*.

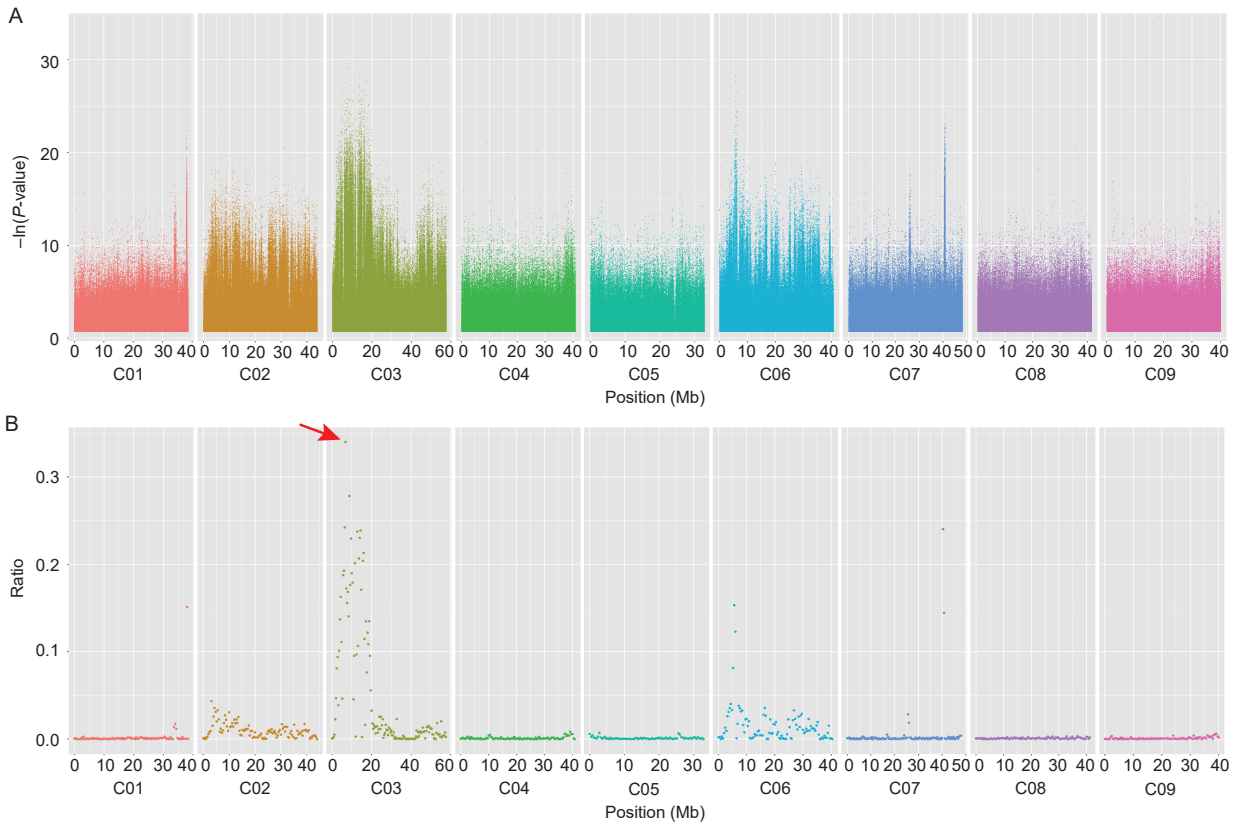


Fig. 3 Manhattan plot of Graded Pool-seq (GPS) for head-splitting resistance. A, *P*-value plot of Ridit analysis before noise-reduction algorithm. B, ratio plot of implementing the strategy of reducing background noise. The *X*-axis is set at a midpoint at each defined genomic interval (~400-kb). The red arrow on chromosome C03 indicates the strongest peak.

undergoing RNA-seq (Appendix B). The analysis generated 556.84 million clean reads, with sample GC content and Q30 exceeding 46 and 93%, respectively (Appendix B). Between 72.42 and 74.53% of the clean reads mapped to the cabbage reference genome (http://brassicadb.cn) (Appendix B).

DEGs were identified by comparing gene expression between ZF and '103' at two heading leaf development time points, as well as between the two time points for each parent. The analysis revealed 204, 4,207, 3,284, and 4,974 DEGs in the four comparison groups: ZF-78 DAP *vs.* ZF-113 DAP, '103'-78 DAP *vs.* '103'-113 DAP, ZF-78 DAP *vs.* '103'-78 DAP, and ZF-113 DAP *vs.* '103'-113 DAP (Fig. 5-A; Appendices C–F). At 78 DAP, 1,690 genes showed significant upregulation and 1,594 genes showed downregulation in the heading leaves of ZF compared to '103' (Fig. 5-B; Appendix E). At 113 DAP, 1,978 genes exhibited increased expression, while 2,996 genes showed decreased expression in the heading leaves of ZF relative to '103' (Fig. 5-C; Appendix F).

GO analysis identified significant terms for the DEGs between ZF and '103' during heading leaf development, with 289 terms at 78 DAP and 338 at 113 DAP. Several terms including GO:0007165 (signal transduction), GO:0009725 (response to hormones), GO:0001101 (response to acid chemicals), and GO:0071310 (cellular response to organic substances) contained substantial numbers of DEGs at both developmental time points (Appendices G and H).

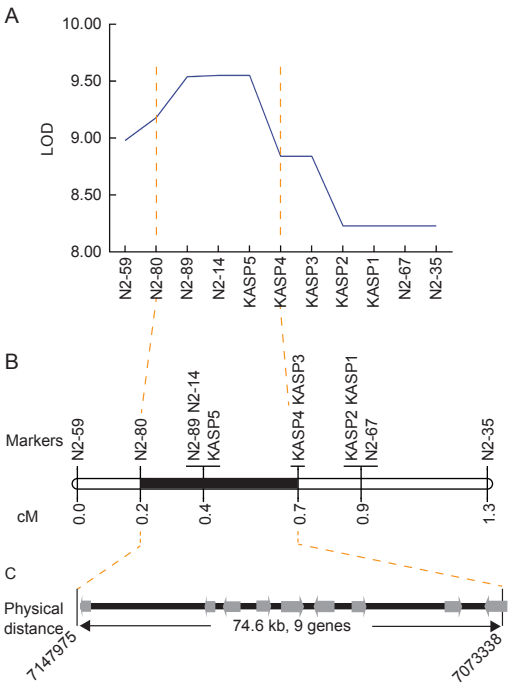


Fig. 4 QTL mapping of head-splitting resistance in *qNLQ3.1*. A, classical QTL analysis in the F_2 population using linkage mapping. B, QTL mapping narrowed down the location of *qNLQ3.1* to an interval flanked by N2-80 and KASP4 markers. C, nine putative genes existed in the 74.6 kb physical distance between the two flank markers.

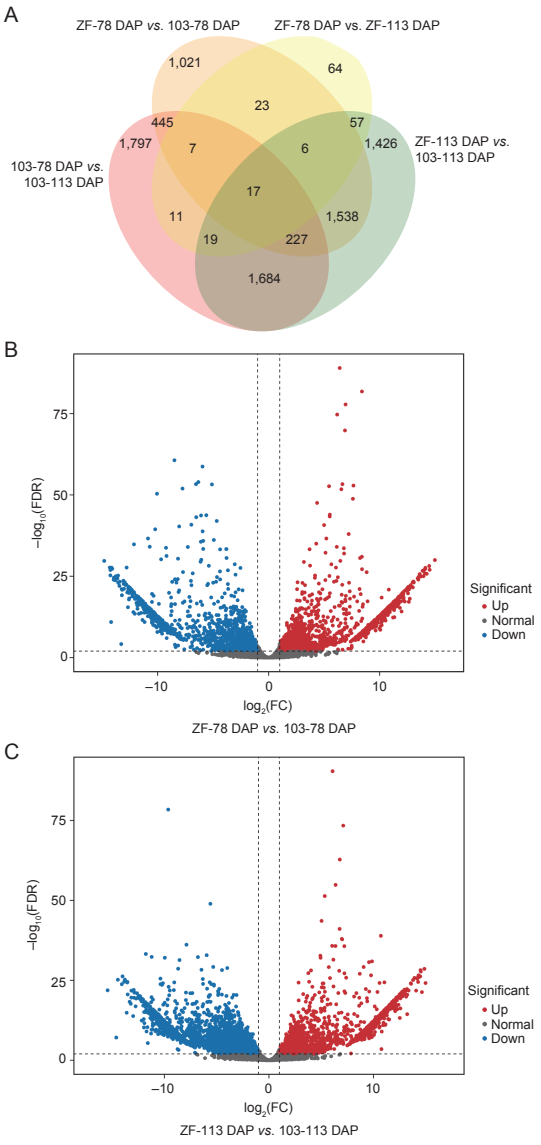


Fig. 5 Differential expression genes (DEGs) at two time points of heading leaf development. A, Venn plot of the number of DEGs between different developmental time points in 'Dazhengfu' (ZF) and '103' and DEGs between two parents at each time point. B, Volcano plot of expressed genes in the heading leaves of ZF and '103' at 78 days after planting (DAP) (ZF-78 DAP *vs.* '103'-78 DAP). C, Volcano plot of expressed genes in the heading leaves of ZF and '103' at 113 DAP (ZF-113 DAP *vs.* '103'-113 DAP). Significant DEGs were labelled by the standard of FDR<0.01 & $|\log_2 FC| \geq 1$, up as red and down as blue, in B and C.

At 78 DAP, five other hormone-related GO terms showed significant enrichment: GO:0060918 (auxin transport), GO:0009926 (auxin polar transport), GO:0009914 (hormone transport), GO:0071368 (cellular response to cytokinin stimulus), and GO:0032870 (cellular response to hormone stimulus) (Appendix G). Meanwhile, another nine hormone-related GO terms were significantly enriched at 113 DAP: GO:0060416 (response to growth hormone), GO:1900458 (negative regulation of brassinosteroid mediated signalling pathway), GO:2000012 (regulation of auxin polar transport), GO:0009690 (cytokinin metabolic process), GO:0009740 (gibberellic acid mediated signalling pathway), GO:0010476 (gibberellin mediated signalling pathway), GO:0071370 (cellular response to gibberellin stimulus), GO:1900457 (regulation of brassinosteroid mediated signalling pathway), and GO:0009787 (regulation of abscisic acid-activated signalling pathway) (Appendix H).

3.7. Hormone metabolite profiling

Based on the potential significance of hormones in regulating cabbage head-splitting resistance, endogenous hormone metabolic profiles were analyzed in ZF and '103' at 78 and 113 DAP, corresponding to the RNA-seq time points. Significant differences in endogenous concentrations of many metabolites in heading leaves of ZF and '103' at 78 and 113 DAP were observed. Among these, the two time points shared 18 kinds of endogenous hormones, with significantly different contents in ZF and '103' (Fig. 6). At 78 DAP, '103' exhibited markedly higher levels of 12 auxins (IAA-Leu, OxIAA, IPA, IAA-Phe, IAA-Glu, IAM, TRP, IAN, Indole, ICAld, MEIAA, and ICA), three CKs (IPR, iP7G, and iPRMP), three JAs (12-OH-JA, JA-Phe, and JA-ILE), and one salicylic acid (SA) (Phe) compared to ZF. Conversely, three CKs (cZ, 2MeScZR, and cZROG), two GAs (GA15 and GA44), one JA (OPC-4), and one SA (SAG) showed markedly lower levels (Fig. 6). Functional analysis indicated that these differential hormone metabolites were associated with 'Phenylalanine, tyrosine, and tryptophan biosynthesis', 'Biosynthesis of various plant secondary metabolites', 'Glucosinolate biosynthesis', 'Biosynthesis of amino acids', and other metabolic pathways (Appendix I). At 113 DAP, '103' displayed significantly higher levels of one auxin (TRP), two CKs (cZROG and iP7G), and one ethylene (ETH) (ACC), while showing significantly reduced levels of eight auxins (IAA-Leu, OxIAA, IPA, IAA, IAN, ICAld, MEIAA, and ICA), seven CKs (IPR, cZ, iP9G, tZRMP, 2MeScZR, cZR, and IP), one GA (GA15), six JAs (JA, OPDA, MEJA, JA-Phe, OPC-4, and JA-ILE) and three SAs (SAG, SA, and MeSAG) (Fig. 6). The differential metabolites were enriched in pathways including 'Plant hormone signal transduction', 'Alpha-Linolenic acid metabolism', 'Zeatin biosynthesis', 'Biosynthesis of cofactor', and others (Appendix I).

These findings were in accordance with the transcriptome analysis results and indicated potential roles for these endogenous hormones in regulating cabbage head-splitting resistance. Furthermore, analysis of hormone-related DEGs between ZF and '103' at both time points revealed five and six distinct groups at 78 and 113 DAP, respectively (Appendices J–L). Notably, genes involved in CK metabolism and signalling pathways constituted the largest group at both time points (48 and 35%, respectively) (Appendices J–L).

3.8. Identification of candidate genes within *qNLQ3.1*

Based on the annotation of the cabbage reference genome, the 74.6 kb candidate interval of *qNLQ3.1* contained nine putative genes (*Bol027992–Bol028000*) (Table 2). Analysis of whole-genome resequencing data from the parental lines revealed six genes with nonsynonymous variants potentially affecting protein function (Appendix M). *Bol027995*, *Bol027996*, *Bol027998*, and *Bol028000*

encoded diacylglycerol O-acyltransferase, ATP-dependent Clp protease ATP-binding subunit ClpX (clpX, CLPX), protein kinase domain (Pkinase), and ethylene-responsive transcription factor CRF3-related proteins, respectively (Table 2). *Bol027992* and *Bol027997* encoded unknown proteins (Table 2).

Among the nine genes within the *qNLQ3.1* interval, three genes showed differential expression during heading leaf development in the RNA-seq analysis (Appendix N). Only one gene, *Bol027999*, demonstrated lower expression across both time points of heading leaf development in '103' compared to ZF; however, its coding sequence showed no nonsynonymous differences between the two parents (Appendices M and N). The expression level of *Bol027997* was significantly elevated in '103' compared to ZF at 113 DAP but not at 78 DAP (Appendix N). *Bol028000* exhibited higher expression at 78 DAP but lower expression at 113 DAP in '103' (Appendix N).

Bol028000 is homologous to Arabidopsis CRF3 and belongs to the APETALA2/Ethylene Response Factor (AP2/ERF) family (Appendix O), in which some members mediate stress responses and developmental programs. Ethylene-responsive factor 4 correlates with rind hardness, providing cracking resistance in fresh watermelon fruits (Liao *et al.* 2020). Additionally, *Bol028000* is physically located on chromosome C03 between 7,146,493 and 7,147,531 bp, adjacent to the peak (*delta* SNP-index=1) of *qNLQ3.1* identified by QTL-seq and contains marker KASP5, where the

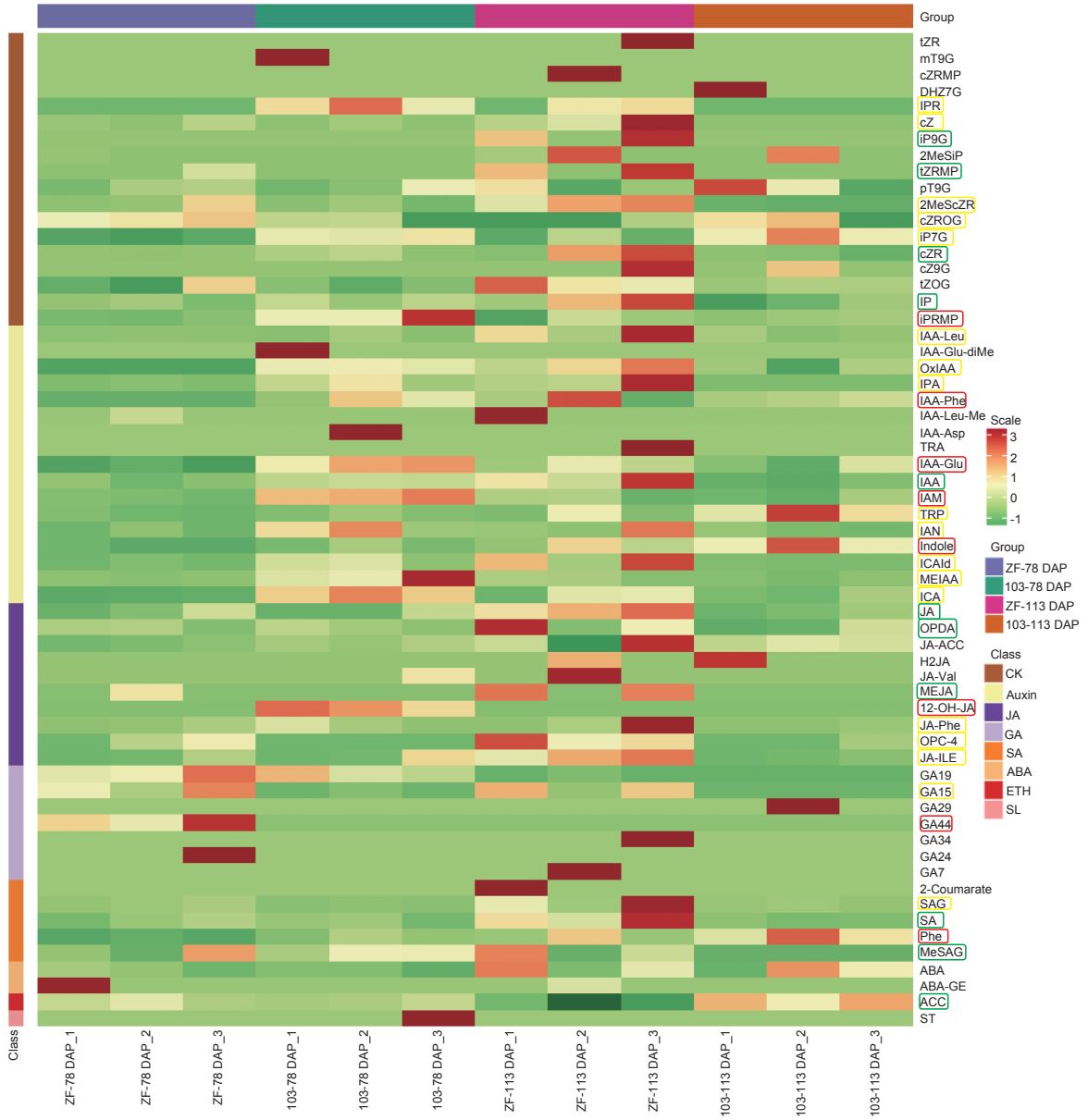


Fig. 6 Heat map depicting endogenous hormone metabolite levels in heading leaves of 'Dazhengfu' (ZF) and '103' at 78 and 113 DAP. Data underwent processing using the unit variance scaling normalization method. Yellow rounded rectangles indicate 18 common endogenous hormones showing significantly different contents between ZF and '103' at 78 and 113 DAP. CK, cytokinin; JA, jasmonic acid; GA, gibberellin; SA, salicylic acid; ABA, abscisic acid; ETH, ethylene; SL, strigolactone.

LOD curve peaked for QTL *qNLQ3.1* (Table 2, Figs. 2-C and 4-A). Therefore, *Bol028000* emerged as the most probable candidate gene for the *qNLQ3.1* locus of cabbage '103'.

To validate this hypothesis, we cloned the *Bol028000* gene from ZF and '103'. The gene contained no introns and exhibited 1,038 bp in '103' and 1,032 bp in ZF in length (Appendix P). Analysis revealed 18 SNPs and two InDels in the exon of *Bol028000* in ZF compared to '103', including eight SNPs and two InDels detected through whole-genome resequencing (Appendices M and P). Among these variations, 11 SNPs and two InDels were nonsynonymous, resulting in 10 amino acid substitutions, three amino acid deletions, and one amino acid insertion (Appendix M; Fig. 7).

Additionally, qRT-PCR was used to confirm the expression level of *Bol028000* in ZF and '103' heading leaves. At 78 and 113 DAP, the expression levels of *Bol028000* were 947.55- and 176.10-fold higher in the head-splitting resistant parent '103' than in the head-splitting susceptible parent ZF, respectively (Fig. 8). Furthermore, the expression in '103' of *Bol028000* at 113 DAP was 5.38-fold lower than at 78 DAP, consistent with the trend observed in its transcriptome data (Fig. 8).

3.9. Subcellular localization

The Bol028000 protein was predicted to localize in the nucleus using the Plant-mPLoc program (Chou and Shen 2010). To experimentally verify its localization, we fused the *Bol028000* coding sequence to the GFP reporter gene driven by the 35S promoter and transiently expressed it in *N. benthamiana* leaves. Fluorescence signals of the Bol028000-GFP fusion protein were detected in the nuclei of *N. benthamiana* epidermal cells, as identified by co-localization with DAPI staining (Fig. 9).

3.10. Allele-specific marker for head-splitting resistance

Among the 11 nonsynonymous SNPs, one SNP at position 768 of *Bol028000* was selected for developing the allele-specific KASP5 marker, which amplified GG alleles in the head-splitting resistant parent '103' and CC alleles in the head-splitting susceptible parent ZF. The KASP5 marker was used to screen 42 inbred lines with previously evaluated head-splitting resistance in Shanghai (Zhu *et al.* 2022). Of the 23 head-splitting resistant lines, 18 displayed GG alleles, four showed CC alleles, and one exhibited a heterozygous pattern, indicating that the KASP5 marker demonstrated 78.3% accuracy in screening resistant lines (Appendices Q and R). Unexpectedly, 12 of the 19 head-splitting susceptible lines also exhibited GG alleles, and one showed a heterozygous pattern (Appendices Q and R). The three head-splitting resistant and 13 head-splitting susceptible lines that could not be identified using the KASP5 marker were genotyped using the established *Bol016058*-based InDel (Zhu *et al.* 2022). The combined use of KASP5 and *Bol016058*-based InDel markers achieved 95.2% successful genotyping across the 23 head-splitting resistant and 19 susceptible lines.

4. Discussion

Head-splitting is economically impactful because of its effects on cabbage production. Despite its significance, understanding of the genetic factors and molecular mechanisms underlying head-splitting resistance in cabbage remains limited. This study integrated multiple QTL mapping methods, transcriptome sequencing, and metabolite profiling to identify genes potentially associated with cabbage head-splitting resistance, providing valuable insights into the molecular mechanisms underlying head-splitting resistance.

Table 2 Gene information in the 74.6 kb candidate interval of *qNLQ3.1*

Gene ID	Position in Chr. C03	Function annotation
Bol027992	7,072,943–7,076,862	Unknown protein
Bol027993	7,078,768–7,080,512	CCT motif family protein
Bol027994	7,100,283–7,101,593	Nuclear migration protein NUDC
Bol027995	7,104,299–7,106,719	Diacylglycerol *O*-acyltransferase
Bol027996	7,106,964–7,110,181	ATP-dependent Clp protease ATP-binding subunit ClpX (clpX, CLPX)
Bol027997	7,111,226–7,112,758	Unknown protein
Bol027998	7,117,028–7,118,989	Protein kinase domain (Pkinase)
Bol027999	7,121,358–7,122,373	Ubiquitin-conjugating enzyme E2 D/E (UBE2D_E, UBC4, UBC5)
Bol028000	7,146,493–7,147,531	Ethylene-responsive transcription factor CRF3-related

The combination of whole-genome resequencing with bulked-segregant analysis (BSA) provides an efficient and effective method for identifying QTLs of interest for crop traits (Takagi *et al.* 2013; Wang *et al.* 2019). This study employed two whole-genome resequencing-based BSA methods (QTL-seq and GPS analysis) to rapidly map the QTLs underlying cabbage head-splitting resistance. Both methods identified a common QTL (*qNLQ3.1*) for head-splitting resistance at the 6.38–9.33 Mb region on chromosome C03 in cabbage (Figs. 2-C and 3-B). To the best of our knowledge, this represents the first reported use of the GPS method in cabbage. The GPS approach offers superior resolution of ~400-kb compared to QTL-seq (Wang *et al.* 2019). The candidate region of *qNLQ3.1* was refined to 0.39 Mb, validated through traditional QTL mapping methods based on genetic linkage analysis (Figs. 3-B and 4-A–C). Previous research identified a large candidate genomic region of 45.8–51.4 Mb (5.6 Mb) on chromosome 3 associated with cabbage head-splitting resistance using only the QTL-seq method with lower mapping resolution (Zhu *et al.* 2022). These findings align with other studies demonstrating the GPS method's efficiency in rapidly mapping major QTLs to precise genomic intervals (Wang *et al.* 2019; Liu J *et al.* 2020; Wen *et al.* 2021; Guan *et al.* 2022; Yue *et al.* 2022; Yuan *et al.* 2023). In 2015, another major QTL named *Hsr 3.2* for cabbage head-splitting resistance was mapped to chromosome C3 (Su *et al.* 2015) and localized near the 5.6 Mb (45.8–51.4 Mb) genomic region previously characterized by Zhu *et al.* (2022). The major QTL (*qNLQ3.1*) detected in this study differs from these previously identified QTLs, suggesting the discovery of a novel genetic locus for head-splitting resistance in cabbage.

Multiple factors, such as water conditions, mineral nutrition, and endogenous hormone content, contribute to head-splitting resistance in cabbage (Zeng *et al.* 2011).



Fig. 7 Alignment of amino acid sequences of Bol028000, Bol028000-Dazhengfu (ZF), and Bol028000-'103'.

Previous research demonstrated that endogenous IAA and GA3 levels are elevated in cabbage head-splitting resistant lines compared to head-splitting susceptible lines during 36–60 DAP at the heading stage (Zeng *et al.* 2009). In the current study, transcriptome analysis revealed that the DEGs between ZF and '103' exhibited significant enrichment in hormone related terms (Appendices G and H). However, the primary hormones regulating head-splitting resistance in '103' remain unidentified. CK represents one of the most crucial plant hormones, promoting morphogenesis while delaying differentiation and senescence to regulate leaf development (Shwartz *et al.* 2016). Furthermore, research indicates CK's potential role in fruit-cracking resistance. Applications of exogenous GA_{4+7} and cytokinin 6-benzyladenine enhance skin resistance to cracking in apples (Joshi *et al.* 2018). Analysis of phytohormone metabolism in *Akebia trifoliata* fruit peels indicates that fruit cracking is accompanied by decreased CK content (Jiang *et al.* 2022). This study's hormone quantification revealed notable differences in several CK forms between ZF and '103' at both 78 and 113 DAP (Fig. 6). Further, we performed correlation analyses between DEGs and differential endogenous hormone metabolites in the two comparison groups: ZF-78 DAP *vs*. '103'-78 DAP, and ZF-113 DAP *vs*. '103'-113 DAP (Appendices K and L). The hormone-related DEGs were most strongly associated with CK metabolism and signalling pathways. These findings collectively suggest CK's role in regulating cabbage head-splitting resistance (Appendix J). Additional systematic studies are required to examine expression changes in genes related to the CK signalling pathway during head-splitting.

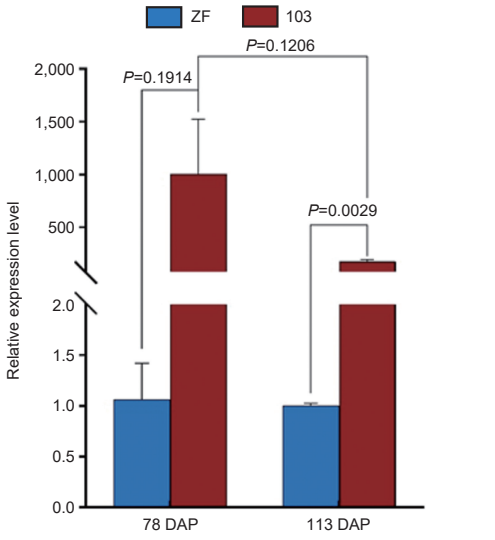


Fig. 8 Expression levels of *Bol028000* as determined by Quantitative RT-PCR (qRT-PCR) between 'Dazhengfu' (ZF) and '103' at 78 and 113 days after planting (DAP). Statistical significance was determined by Student's *t*-test. The expression of cabbage *Actin* gene was used for the normalization control. Error bars indicate SE.

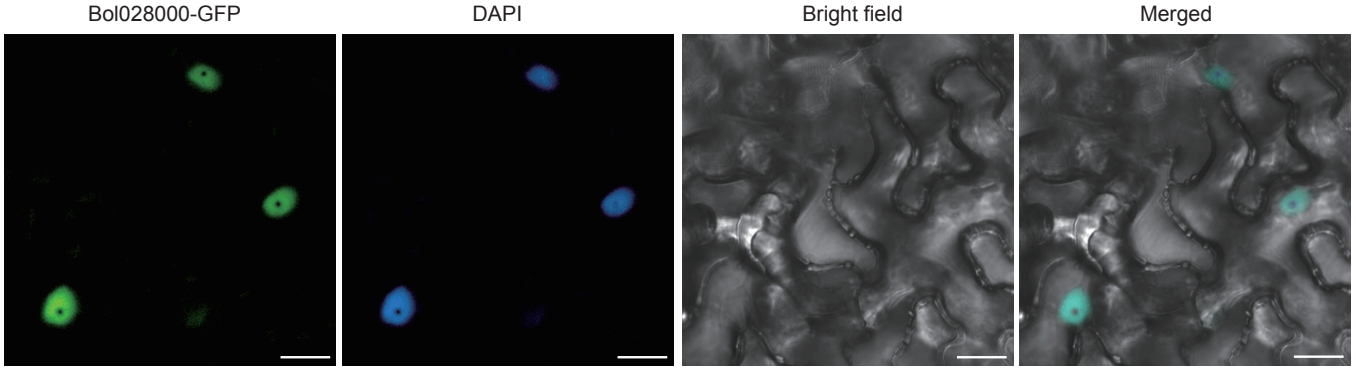


Fig. 9 Subcellular localization of Bol028000-green fluorescent protein (GFP) fusion protein in epidermal cells of *Nicotiana benthamiana* leaves. Scale bars=50 μm.

A comprehensive database is now available at http://phgd.bio2db.com/ to facilitate plant hormone pathway and mechanism studies (Feng *et al.* 2024a, b).

CRFs, a subfamily of AP2/ERF transcription factors, function as a side branch of the two-component signalling pathway that modulates cytokinin-regulated target genes (Rashotte *et al.* 2006). Through sequence-based functional annotation, this study identified *Bol028000*, which encodes a protein homologous to *Arabidopsis* CRF3 (Table 2; Appendix O), as a head-splitting resistance facilitator with sequence polymorphism (Fig.7; Appendix P) and differential expression levels (Fig. 8) between head-splitting resistant line '103' and susceptible line ZF. Evidence suggests certain CRF members' involvement in leaf development. Arabidopsis CRF6 negatively regulates leaf senescence in dark-induced senescence assays of excised leaves, affecting the transition to reproductive development (Zwack *et al.* 2013). The Arabidopsis *crf1*,*3*,*5*,*6* and *crf1/CRF1*,*2*,*5*,*6* mutant lines demonstrate delayed senescence, while *CRF1*, *CRF3*, and *CRF5* overexpression lines show early leaf senescence in intact plants (Raines *et al.* 2016). Additionally, the regulation of the expression of genes involved in cytokinin and other hormone metabolism in the *crf1*,*3*,*5*,*6* mutant suggests that disruption of CRFs results in a complex effect on phytohormone levels (Raines *et al.* 2016). Recent research shows that *SlCRF6* overexpression in tomatoes inhibits leaf development through the GA signalling pathway (Liao *et al.* 2024). Further investigation is needed to understand how *Bol028000* regulates cabbage head-splitting resistance.

Significantly, the previously reported head-splitting resistance marker *Bol016058*-based InDel shows no polymorphism between ZF and '103' (Zhu *et al.* 2022). This study developed a functional marker based on one nonsynonymous SNP of *Bol028000*, KASP5, and combined applications of the *Bol016058*-based InDel (Zhu *et al.* 2022) and KASP5 markers (Appendices Q and R) in 42 breeding lines, achieving 95.2% accuracy. These findings may facilitate the improvement of head-splitting resistance in cabbage plants.

5. Conclusion

In this study, one major QTL controlling head-splitting resistance, *qNLQ3.1*, was mapped to a 74.6 kb physical region on chromosome C03 using multiple approaches including QTL-seq, GPS, and traditional genetic linkage analysis. The integration of transcriptomic and metabolic profiling facilitated the elucidation of nine putative genes located within the mapped genetic region. The implementation of newly developed KASP markers for head-splitting resistance could enhance genotyping and selection efficiency. These findings advance our understanding of the genetic architecture underlying cabbage head-splitting resistance.

Acknowledgements

This research was funded by the Agricultural Development Program through Science and Technology of Shanghai, China (2022-02-08-00-12-F01099), the National Key R&D Program of China (2023YFD1201501), the Science and Technology Commission of Shanghai Municipality, China (22DX1900100), and the Excellent Team Project of Shanghai Academy of Agricultural Sciences, China (2022(007)).

Declaration of competing interest

The authors declare that they have no conflict of interest.

Declaration of generative AI and AI-assisted technologies in the writing process

The authors declare that they did not use AI in the preparation and writing of this manuscript.

Appendices associated with this paper are available at https://doi.org/10.1016/j.jia.2025.11.020

References

Alemán-Báez J, Qin J, Cai C, Zou C, Bucher J, Paulo M J, Voorrips R E, Bonnema G. 2022. Genetic dissection of morphological variation in rosette leaves and leafy heads in cabbage (*Brassica oleracea* var. *capitata*). *Theoretical and Applied Genetics*, **135**, 3611–3628.

Bar M, Ori N. 2014. Leaf development and morphogenesis. *Development*, **141**, 4219–4230.

Cheng F, Sun R, Hou X, Zheng H, Zhang F, Zhang Y, Liu B, Liang J, Zhuang M, Liu Y, Liu D, Wang X, Li P, Liu Y, Lin K, Bucher J, Zhang N, Wang Y, Wang H, Deng J, *et al.* 2016. Subgenome parallel selection is associated with morphotype diversification and convergent crop domestication in *Brassica rapa* and *Brassica oleracea*. *Nature Genetics*, **48**, 1218–1224.

Chiang M S. 1972. Inheritance of head splitting in cabbage (*Brassica oleracea* L. var. *capitata* L.). *Euphytica*, **21**, 507–509.

Chou K C, Shen H B. 2010. Plant-mPLoc: A top-down strategy to augment the power for predicting plant protein subcellular localization. *PLoS ONE*, **5**, e11335.

Du F, Guan C, Jiao Y. 2018. Molecular mechanisms of leaf morphogenesis. *Molecular Plant*, **11**, 1117–1134.

Feng S, Liu Z, Chen H, Li N ,Yu T, Zhou R, Nie F, Guo D, Ma X, Song X. 2024a. PHGD: An integrative and user-friendly database for plant hormone related genes. *iMeta*, **3**, e164.

Feng S, Li N, Chen H, Liu Z, Li C, Zhou R, Zhang Y, Cao R, Ma X, Song X. 2024b. Large-scale analysis of the ARF and Aux/IAA gene families in 406 horticultural and other plants. *Molecular Horticulture*, **4**, 13.

Gao L W, Lyu S W, Tang J, Zhou D Y, Bonnema G, Xiao D, Hou X L, Zhang C W. 2017. Genome-wide analysis of auxin transport genes identifies the hormone responsive patterns associated with leafy head formation in Chinese cabbage. *Scientific Reports*, **7**, 42229.

Gao Y, Huang S, Qu G, Fu W, Zhang M, Liu Z, Feng H. 2020. The mutation of ent-kaurene synthase, a key enzyme involved in gibberellin biosynthesis, confers a non-heading phenotype to Chinese cabbage (*Brassica rapa* L. ssp. pekinensis). *Horticulture Research*, **7**, 178.

Guan J, Li J, Yao Q, Liu Z, Feng H, Zhang Y. 2022. Identification of two tandem genes associated with primary rosette branching in flowering Chinese cabbage. *Frontiers in Plant Science*, **13**, 1083528.

He Y K, Xue W X, Sun Y D, Yu X H, Liu P L. 2000. Leafy head formation of the progenies of transgenic plants of Chinese cabbage with exogenous auxin genes. *Cell Research*, **10**, 151–160.

Huang S, Gao Y, Xue M, Xu J, Liao R, Shang S, Yang X, Zhao Y, Li C, Liu Z, Feng H. 2022. *BrKAO2* mutations disrupt leafy head formation in Chinese cabbage (*Brassica rapa* L. ssp. *pekinensis*). *Theoretical and Applied Genetics*, **135**, 2453–2468.

Jiang Y, Yin H, Wang D, Zhong Y, Deng Y. 2022. Exploring the mechanism of *Akebia trifoliata* fruit cracking based on cell-wall metabolism. *Food Research International*, **157**, 111219.

Joshi M, Baghel R S, Fogelman E, Stern R A, Ginzberg I. 2018. Identification of candidate genes mediating apple fruit-cracking resistance following the application of gibberellic acids 4 + 7 and the cytokinin 6-benzyladenine. *Plant Physiology and Biochemistry*,

127, 436–445.
Kim D, Langmead B, Salzberg S L. 2015. HISAT: A fast spliced aligner with low memory requirements. *Nature Methods*, **12**, 357–360.
Li H, Durbin R. 2009. Fast and accurate short read alignment with Burrows–Wheeler transform. *Bioinformatics*, **25**, 1754–1760.
Li L C, Kang D M, Chen Z L, Qu L J. 2007. Hormonal regulation of leaf morphogenesis in *Arabidopsis*. *Journal of Integrative Plant Biology*, **49**, 75–80.
Liao C, Shen H, Gao Z, Wang Y, Zhu Z, Xie Q, Wu T, Chen G, Hu Z. 2024. Overexpression of *SlCRF6* in tomato inhibits leaf development and affects plant morphology. *Plant Science*, **338**, 111921.
Liao N, Hu Z, Li Y, Hao J, Chen S, Xue Q, Ma Y, Zhang K, Mahmoud A, Ali A, Malangisha G K, Lyu X, Yang J, Zhang M. 2020. *Ethylene-responsive factor 4* is associated with the desirable rind hardness trait conferring cracking resistance in fresh fruits of watermelon. *Plant Biotechnology Journal*, **18**, 1066–1077.
Liu J, Gong J, Wei X, Yang S, Huang X, Li C, Zhou X, 2020. Dominance complementation of *Hd1* and *Ghd8* contributes to extremely late flowering in two rice hybrids. *Molecular Breeding*, **40**, 76.
Liu X, Zhao C, Yang L, Zhuang M, Zhang Y, Wang Y, Fang Z, Lv H. 2020. A time-resolved dual transcriptome analysis reveals the molecular regulating network underlying the compatible/incompatible interactions between cabbage (*Brassica oleracea*) and *Fusarium oxysporum* f. sp. *conglutinans*. *Plant Soil*, **448**, 455–478.
McKenna A, Hanna M, Banks E, Sivachenko A, Cibulskis K, Kernytsky A, Garimella K, Altshuler D, Gabriel S, Daly M, DePristo M A. 2010. The Genome Analysis Toolkit: A MapReduce framework for analyzing next-generation DNA sequencing data. *Genome Research*, **20**, 1297–1303.
Van Ooijen W, van Ooijen J, van't Verlaat J, tol J, Dalen J, Van Ooijen J W, van Ooijen J W, Kyazma B V, Ooijen J, Van J, Van Oojien J, Van Ooijen J, Kyazmay B, Riel J, Camp N, Van Ooijen, Ooijen J V, Verlaat J G, Tol J L, Kyazma B, *et al*. 2006. *Joinmap®4: Software for the Calculation of Genetic Linkage Maps in Experimental Population*. Kyazma BV, Wagenigen.
Van Ooijen J, Ooijen W V, van J, Ooijen J, Hoorn J, Van Duin J, Van Ooijen J, Van Ooijen J W, Van J, Van Ooijen J W, van Ooijen J, Van Ooijen J W, Ooijen J W, Hoorn J W, Duin J, van't Verlaat J W. 2009. *MapQTL®6. Software for the Mapping of Quantitative Trait Loci in Experimental Populations of Diploid Species*. Kyazma BV, Wagenigen.
Pang W, Li X, Choi S R, Nguyen V D, Dhandapani V, Kim Y Y, Ramchiary N, Kim J G, Edwards D, Batley J, Na J, Kim H R, Lim Y P. 2015. Mapping QTLs of resistance to head splitting in cabbage (*Brassica oleracea* L. var. *capitata* L.). *Molecular Breeding*, **35**, 126.
Pertea M, Pertea G M, Antonescu C M, Chang T C, Mendell J T, Salzberg S L. 2015. StringTie enables improved reconstruction of a transcriptome from RNA-seq reads. *Nature Biotechnology*, **33**, 290–295.
Raines T, Shanks C, Cheng C Y, McPherson D, Argueso C T, Kim H J, Franco-Zorrilla J M, López-Vidriero I, Solano R, Vaňková R, Schaller G E, Kieber J J. 2016. The cytokinin response factors modulate root and shoot growth and promote leaf senescence in Arabidopsis. *Plant Journal*, **85**, 134–147.
Rashotte A M, Mason M G, Hutchison C E, Ferreira FJ, Schaller G E, Kieber J J. 2006. A subset of *Arabidopsis* AP2 transcription factors mediates cytokinin responses in concert with a two-component pathway. *Proceedings of the National Academy of Sciences of the United States of America*, **103**, 11081–11085.
Shwartz I, Levy M, Ori N, Bar M. 2016. Hormones in tomato leaf development. *Developmental Biology*, **419**, 132–142.
Su Y, Li Q, Yi D, Liu L, Fu C, Zhang T, Zhang H, Chen Y. 2019. Genetic analysis of traits related to head in white cabbage. *Northern Horticulture*, **8**, 7–14. (in Chinese)
Su Y, Liu Y, Fang Z, Yang L, Zhuang M, Zhang Y, Zhang X, Sun P. 2012. Genetic analysis of head-splitting resistance traits in cabbage. *Acta Horticulturae Sinica*, **39**, 1482–1490. (in Chinese)
Su Y, Liu Y, Li Z, Fang Z, Yang L, Zhuang M, Zhang Y. 2015. QTL analysis of head splitting resistance in cabbage (*Brassica oleracea* L. var. *capitata*) using SSR and InDel makers based on whole-genome re-sequencing. *PLoS ONE*, **10**, e0138073.
Sun X, Basnet R K, Yan Z, Bucher J, Cai C, Zhao J, Bonnema G. 2019. Genome-wide transcriptome analysis reveals molecular pathways involved in leafy head formation of Chinese cabbage (*Brassica rapa*). *Horticulture Research*, **6**, 130.
Tabusam J, Liu M, Luo L, Zulfiqar S, Shen S, Ma W, Zhao J. 2023. Physiological control and genetic basis of leaf curvature and heading in *Brassica rapa* L. *Journal of Advanced Research*, **53**, 49–59.
Takagi H, Abe A, Yoshida K, Kosugi S, Natsume S, Mitsuoka C, Uemura A, Utsushi H, Tamiru M, Takuno S, Innan H, Cano LM, Kamoun S, Terauchi R. 2013. QTL-seq: Rapid mapping of quantitative trait loci in rice by whole genome resequencing of DNA from two bulked populations. *Plant Journal*, **74**, 174–183.
Wang C, Tang S, Zhan Q, Hou Q, Zhao Y, Zhao Q, Feng Q, Zhou C, Lyu D, Cui L, Li Y, Miao J, Zhu C, Lu Y, Wang Y, Wang Z, Zhu J, Shangguan Y, Gong J, Yang S, *et al.* 2019. Dissecting a heterotic gene through GradedPool-Seq mapping informs a rice-improvement strategy. *Nature Communications*, **10**, 2982.
Wen T, Liu C, Wang T, Wang M, Tang F, He L. 2021. Genomic mapping and identification of candidate genes encoding nulliplex-branch trait in sea-island cotton (*Gossypium barbadense* L.) by multi-omics analysis. *Molecular Breeding*, **41**, 34.
Yu G, Wang L G, Han Y, He Q Y. 2012. clusterProfiler: An R package for comparing biological themes among gene clusters. *Omics*, **16**, 284–287.
Yuan G, Li Y, He D, Shi J, Yang Y, Du J, Zou C, Ma L, Pan G, Shen Y. 2023. A combination of QTL mapping and GradedPool-Seq to dissect genetic complexity for Gibberella ear rot resistance in maize using an IBM Syn10 DH population. *Plant Disease*, **107**, 1115–1121.
Yue L, Sun R, Li G, Cheng F, Gao L, Wang Q, Zhang S, Zhang H, Zhang S, Li F. 2022. Genetic dissection of heterotic loci associated with plant weight by Graded pool-seq in heading Chinese cabbage (*Brassica rapa*). *Planta*, **255**, 126.
Zeng A, Liu Y, Fang Z, Yan J. 2011. Research progress of head splitting on cabbage (*Brassica oleracea* L. var. *capitata* L.). *Journal of Plant Genetic Resources*, **12**, 307–310.
Zeng A, Liu Y, Fang Z, Yang L, Zhuang M, Zhang Y, Sun J, Sun P. 2009. Relationship between endogenous hormone contents and head-splitting character during *Brassica oleracea* L. var. *capitata* L. vegetative period. *China Vegetables*, **20**, 11–16. (in Chinese)
Zhang K, Yang Y, Wu J, Liang J, Chen S, Zhang L, Lv H, Yin X, Zhang X, Zhang Y, Zhang L, Zhang Y, Freeling M, Wang X, Cheng F. 2022. A cluster of transcripts identifies a transition stage initiating leafy head growth in heading morphotypes of *Brassica*. *Plant Journal*, **110**, 688–706.
Zhang X, Ma W, Liu M, Li X, Li J, Lu Y, Li G, Zhang S, Feng D, Wang Y, Liang H, Luo S, Li N, Gu A, Xuan S, Chen X, Shen S, Zhao J. 2022. OCTOPUS regulates BIN2 to control leaf curvature in Chinese cabbage. *Proceedings of the National Academy of Sciences of the United States of America*, **119**, e2208978119.
Zhao B, Liu Q, Wang B, Yuan F. 2021. Roles of phytohormones and their signaling pathways in leaf development and stress responses. *Journal of Agricultural and Food Chemistry*, **69**, 3566–3584.
Zhu X, Chen J, Tai X, Wang M, Ren Y, Bo T. 2023. Fine mapping and identification of the candidate gene *BoPur* for purple head trait in cabbage (*Brassica oleracea* var. *capitata*). *Plant Breeding*, **142**, 537–546.
Zhu X, Tai X, Ren Y, Wang M, Chen J, Bo T. 2022. QTL-seq and marker development for resistance to head splitting in cabbage. *Euphytica*, **218**, 41.
Zwack P J, Robinson B R, Risley M G, Rashotte A M. 2013. Cytokinin response factor 6 negatively regulates leaf senescence and is induced in response to cytokinin and numerous abiotic stresses. *Plant and Cell Physiology*, **54**, 971–981.

Executive Editor-in-Chief Sanwen Huang
Managing Editor Lingyun Weng